

Suitability of High Temperature and High Strain Rate Superplastic Deep Drawing Process for AA5052 Alloy

Chennakesava R Alavala

Abstract— In the present work, the suitability of high temperature and high strain rate deep drawing process was assessed for AA5052 aluminum alloy. The assessment was carried out using Taguchi technique and finite element analysis. The process parameters were temperature, strain rate, coefficient of friction and blank holder velocity. The formability limit diagrams were drawn for all the trials.

Index Terms— AA5052 alloy, superplastic deep drawing process, high temperature, high strain rate, coefficient of friction, cylindrical cups, forming limit diagram.

I. INTRODUCTION

The design and control of a deep drawing process depends not only on the workpiece material, but also on the condition at the tool- workpiece interface and the mechanics of plastic deformation. There are many researches [1-4] focus on the effects of process or material parameters on the on deep drawing process. During the design of deep drawing processes, numerical simulation which can predicate material flow trend, stress and strain distribution, can help to determine the optimal processing parameters and explore the possibility high temperature and high strain rate (HTHSR) deep drawing process [5-12].

In this paper, finite element method software, namely, DEFORM-3D is used to simulate the cylindrical cup deep drawing of AA5052 alloy sheet at elevated temperatures and strain rates. A finite element method is also used to investigate the effective stress and forming limit diagram under various process parameters such as such as blank thickness, temperature, strain rate and coefficient of friction.

Table 1. Control parameters and levels.

Factor	Symbol	Level-1	Level-2	Level-3
Temperature, °C	A	300	400	500
Strain rate, 1/s	B	0.1	0.5	1.0
Coefficient of friction	C	0.1	0.15	0.2
Blank holder velocity, mm/s	D	0.13	0.17	0.20

II. MATERIAL AND METHODS

In the present work, AA5052 alloy was used to make cylindrical cups. The levels chosen for the controllable process parameters are summarized in table 1. Each of the process parameters was planned at three levels. The orthogonal array (OA), L9 was chosen to carry out experimental and finite element analysis (FEA). The requirement of parameters in the OA matrix is given in table 2.

Table 2. Orthogonal array (L9) and control parameters

Treat No.	A	B	C	D
1	1	1	1	1
2	1	2	2	2
3	1	3	3	3
4	2	1	2	3
5	2	2	3	1
6	2	3	1	2
7	3	1	3	2
8	3	2	1	3
9	3	3	2	1

The finite element modeling and analysis was acknowledged using D-FORM 3D software. The cylindrical sheet blank was created with desired diameter and thickness using CAD tools. The sheet blank was meshed with tetrahedral elements [13]. The cylindrical top punch, cylindrical bottom hollow die were also modeled with appropriate inner and outer radius and corner radius using CAD tools (Fig. 1). The mechanical interface between the contact surfaces was implicated to be frictional contact and modeled as Coulomb's friction model [8-11].

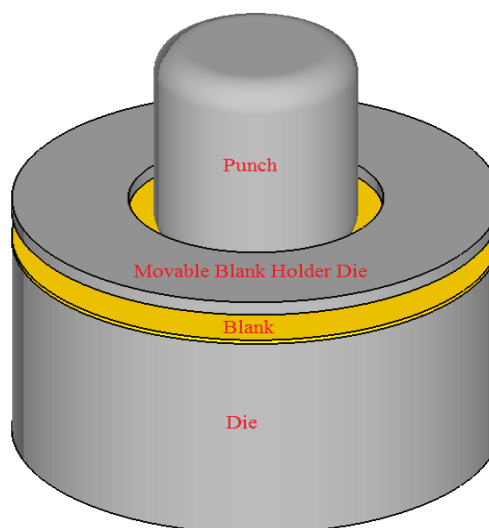


Fig. 1. Cylindrical cup drawing without blank holder die.

III. RESULTS AND DISCUSSION

In the present work, the significance of process parameters which had an absolute Fisher's ratio larger than 3.4579 (at least 90% of confidence) were believed to influence the average value for the forming characteristic under null hypothesis.

A. Influence of Process Parameters on Effective Stress

The sufficiency of the finite element analysis was excellent as the percent contribution due to error was zero. In table 3, the percent contribution indicates that the parameter C, coefficient of friction, all by itself enriches two-third of the variation in the effective stress: almost 67.81%. The temperature (A) renders into a one-fourth of the variation (24.56%) in the effective stress. The influence of strain rate (B) and blank holder velocity (D) was very small. It was observed that only three results (1/3 of the experiments) were higher than the average effective stress. Hence, only two process parameters could influence the effective stress.

Table 3. ANOVA summary of the effective stress

Source	Sum 1	Sum 2	Sum 3	SS	v	V	F	P
A	1392.41	1707.88	1583.56	16835.94	1	16835.94	14016747.00	24.56
B	1487.08	1573.19	1623.59	3176.53	1	3176.53	2644617.25	4.63
C	1865.69	1424.48	1393.68	46489.16	1	46489.16	38704509.17	67.81
D	1501.09	823906.93	4683.85	2057.97	1	2057.97	1713361.11	3.00
e				2057.97	1	2057.97	1.00	0
T	6246.26	828612.49	9284.68	0.0048	4	0.0012		100

Note: SS is the sum of square, v is the degrees of freedom, V is the variance, F is the Fisher's ratio, P is the percentage of contribution and T is the sum squares due to total variation.

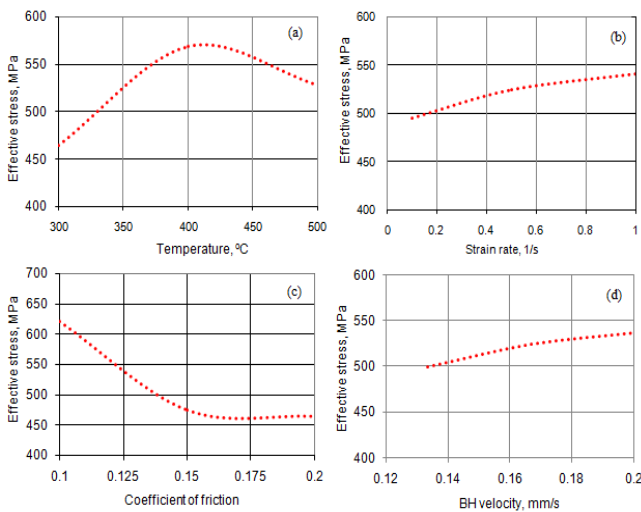


Fig. 2. Effect of process parameters on the effective stress: (a) temperature, (b) strain rate, (c) coefficient of friction and (d) blank holder velocity.

Fig. 2(a) presents the effective stress induced in AA3003 alloy during cup drawing process as a function of temperature. The effective stress was higher at temperature 400°C as compared to other two temperatures: 300°C and 500°C. However, the stress induced at temperature 500°C was higher than that induced at 300°C. Fig. 2(b) describes the effective stress as a function of strain rate. The effective stress increased with the increase strain rate. But, the effective stress decreased with the increase of friction coefficient during the deep drawing process as showed in Fig 2(c). Fig. 2(d) describes the effective stress as a function of movable blank holder velocity. The effective stress increases with the increase of the blank holder velocity.

The FEA results of effective stress are showed in Fig. 3 for various test conditions as per the design of experiments. For trials 1, 2 and 3, the temperature was 300°C and other process parameters were varied as mentioned in tables 1 and 2. The maximum effective stresses for trails 1, 2 and 3 were, respectively, 520.80 MPa, 426.13 MPa and 645.47 MPa. For trials 4, 5 and 6, the temperature was 400°C and other process parameters were as stated in tables 1 and 2. The effective stresses for trails 4, 5 and 6 were, respectively, 515.39 MPa, 497.33MPa and 695.16 MPa. For trials 7, 8 and 9, the temperature was 500°C and other process parameters were as designed in tables 1 and 2. The effective stresses for trails 7, 8 and 9 were, respectively, 450.88 MPa, 649.73 MPa and 482.96 MPa. It is also observed that the effective stress decreases with the increase of temperature (Fig.4).

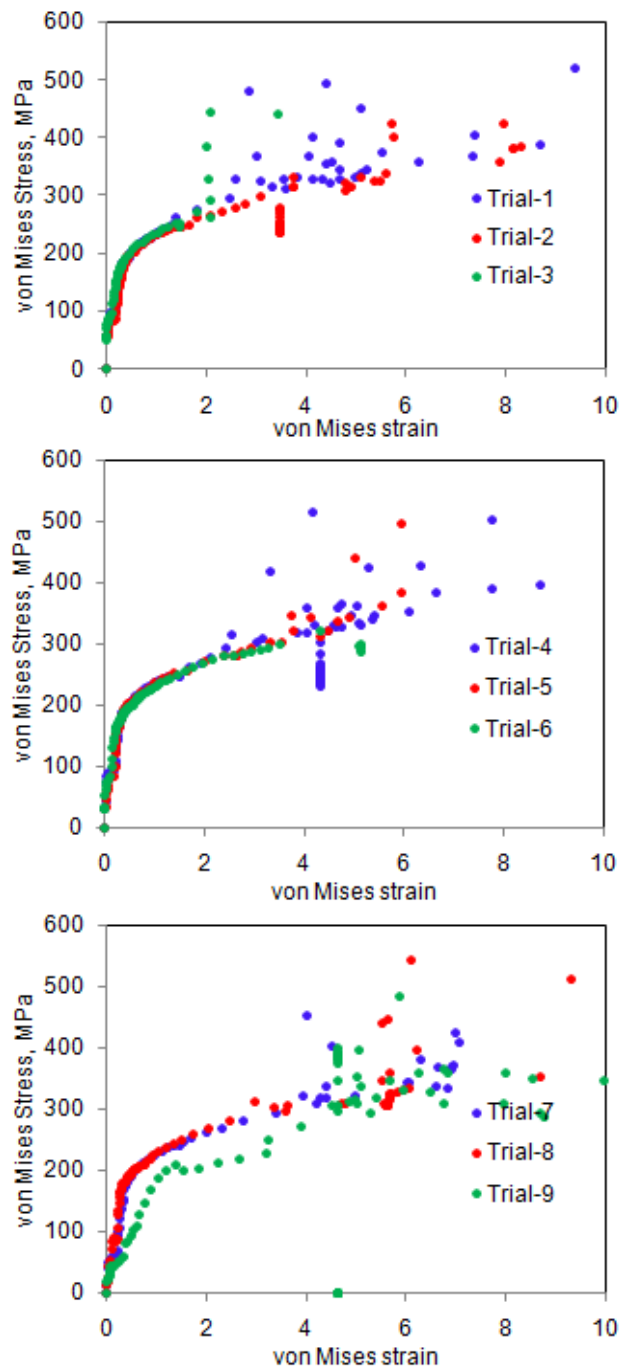


Fig. 3. Effect of process parameters on the effective stress.

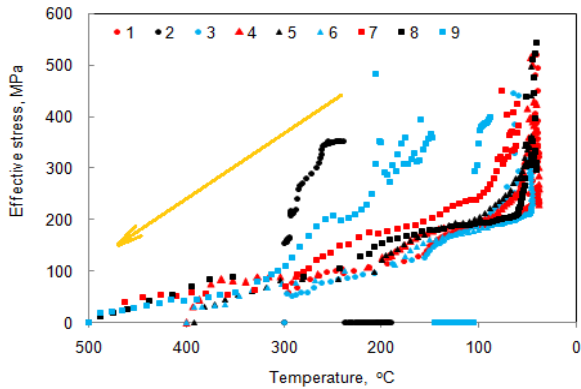


Fig. 4. Effect of temperature on the effective stress.

B. Influence of process parameters on surface expansion ratio

The relative influences of process parameters are summarized in table 4. If the percent contribution due to error is low (10% or less), then it is assumed that no important factors were omitted from the experiment. In table 4, the percent contribution indicates that the parameter C, coefficient of friction, all by itself accords two-third (67.14%) of the total variation in the surface expansion ratio. In the order of merits, blank holder velocity, temperature and strain rate would contribute, respectively, 13.26%, 11.83% and 7.77% towards the total variation in the surface expansion ratio. Of all nine results, two results are higher than the average surface expansion ratio. Hence, two or three process parameters would dominant in controlling the surface expansion ratio. The strongest process parameters were coefficient of friction, blank holder velocity and temperature in their order of strongest.

Table 4. ANOVA summary of the surface expansion ratio

Source	Sum 1	Sum 2	Sum 3	SS	v	V	F	P
A	67.00	41.43	125.50	1238.2	1	1238.2	2913411.76	11.83
B	45.88	72.90	115.15	812.61	1	812.61	1912023.53	7.77
C	6.51	195.60	31.82	7024.39	1	7024.39	16527976.46	67.14
D	124.68	1911.68	233.93	1387.55	1	1387.55	3264823.53	13.26
e				0.0017	4	0.000425	1.00	0
T	244.07	2221.61	506.40	10462.752	8			100

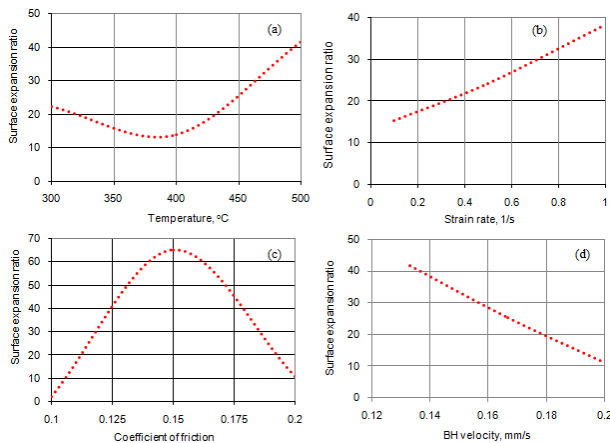


Fig. 5. Effect of process parameters on the surface expansion ratio: (a) temperature, (b) strain rate, (c) coefficient of friction and (d) blank holder velocity.

The surface expansion ratio was very high for the temperature of 500°C and for the coefficient of friction at 0.15 as illustrated in Fig. 5a and 5b, respectively. The surface expansion ratio increased with the increase of strain rate as shown in Fig 5(b). The surface expansion ratio decreased with the increase of blank holder velocity (Fig. 5d). This is true because high blank holder velocity would restrain the free flow of material into the die and subsequently the deformation process.

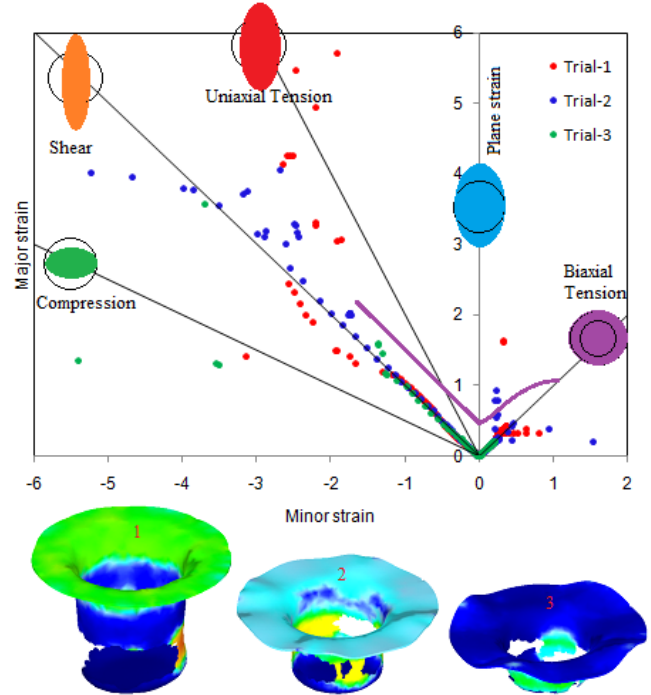


Fig. 6. Forming limit diagram with damages in the cups drawn at temperature 300°C.

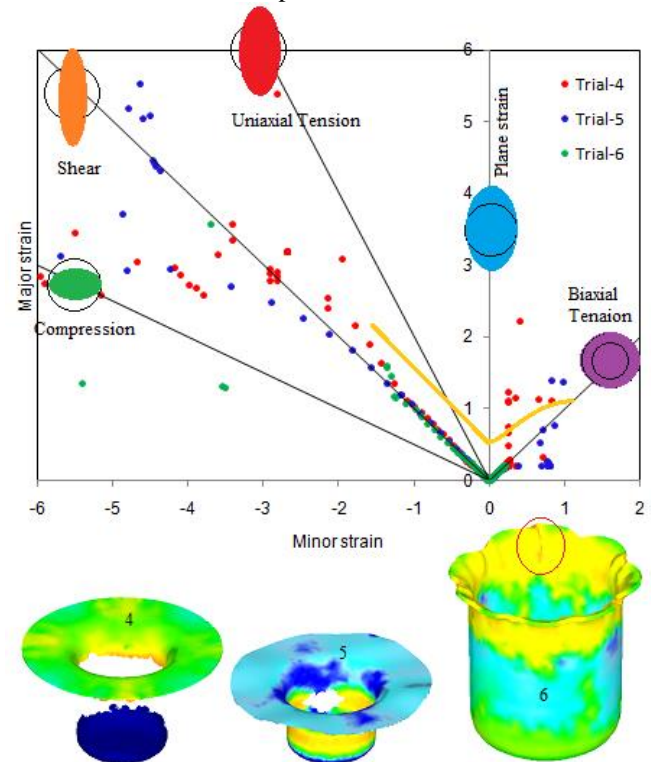


Fig.7. Forming limit diagram with damage in the cups drawn at temperature 400°C.

C. Forming limit diagrams and damages in the cups

Fig. 6 depicts the forming limit diagram (FLD) with damages in the cylindrical cups drawn from AA5052 alloy sheets at temperature 300°C. The FLD for the cylindrical cup drawn with trial 1 was ruptured because of both uniaxial and biaxial tensions. The fracture has occurred in the cups drawn with trial 2 due to shear and equi-biaxial tension. For cups drawn with trial 3, the fracture was due compression and shear. Fig. 7 demonstrates the forming limit diagram and damages in the cups drawn from AA5052 alloy sheets with trials, 4, 5 and 6 at temperature 400°C. Cups drawn on trials 4 and 5 were damaged on account of compression, shear and biaxial tensions. Cups drawn from trials 5 were ruptured due to uniaxial tension. The fracture was observed in the flange area of the cups drawn with trail 6 due to uniaxial compression of blank between die and movable blank holder. Fig. 8 demonstrates the FLD and damages in the cups drawn from AA5052 alloy sheets with trials, 7, 8 and 9 at temperature 500°C. Cups drawn from trials 7 and 9 were experienced fracture due to uniaxial tension and shear. Cups drawn under trial 8 were not fractured.

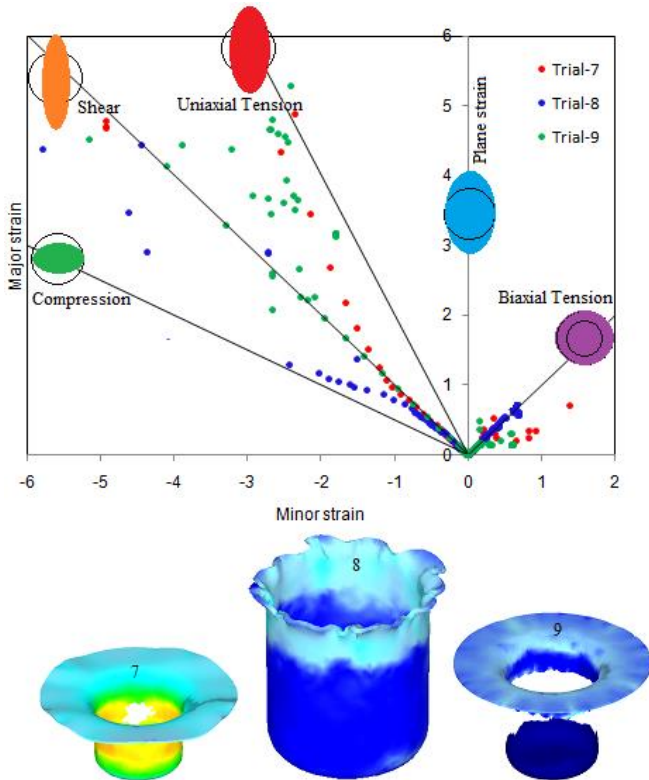


Fig. 8. Forming limit diagram with damage in the cups drawn at temperature 500°C.

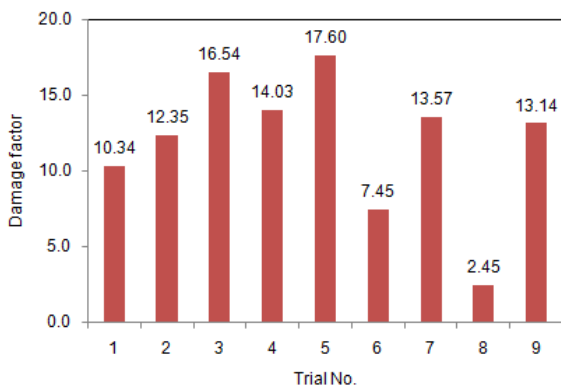


Fig. 9. Damage factors under different trials.

The damages of cups drawn from all trials are showed in Fig. 9. The damage of cups was very lower for the cup drawn from trial 8 as compared with the rest of 8 trials. The damage was also small but it was happened during the last stages of deep drawing process.

IV. CONCLUSIONS

With strain rate of 0.5 s⁻¹, temperature of 500°C, coefficient of friction of 0.1, and blank holder velocity of 0.2 mm/s could yield damageless cups (trial 8). Therefore, high temperature and high strain rate (HTHSR) deep drawing is prospective to draw cups from AA5052 alloy.

REFERENCES

- [1] R. Hill, A theory of the yielding and plastic flow of anisotropic metals, Proceedings of Royal Society of London, 1948, 193-281.
- [2] Y.Q. Liu, J.C. Wang, P. Hu, The numerical analysis of anisotropic sheet in deep-drawing processes, Journal of Materials Processing Technology 120, 2002, 45-52.
- [3] A. C. Reddy, "Homogenization and Parametric Consequence of Warm Deep Drawing Process for 1050A Aluminum Alloy: Validation through FEA," International Journal of Science and Research, 4(4), 2015, 2034-2042.
- [4] A. C. Reddy, "Finite element analysis of reverse superplastic blow forming of Ti-Al-4V alloy for optimized control of thickness variation using ABAQUS," Journal of Manufacturing Engineering, 1(1), 2006, 6-9.
- [5] K. Chandini, A. C. Reddy, "Parametric Importance of Warm Deep Drawing Process for 1070A Aluminium Alloy: Validation through FEA," International Journal of Scientific & Engineering Research, 6(4), 2015, 399-407.
- [6] B. Yamuna, A. C. Reddy, "Parametric Merit of Warm Deep Drawing Process for 1080A Aluminium Alloy: Validation through FEA," International Journal of Scientific & Engineering Research, 6(4), 2015, 416-424.
- [7] T. Srinivas, A. C. Reddy, "Parametric Optimization of Warm Deep Drawing Process of 1100 Aluminum Alloy: Validation through FEA," International Journal of Scientific & Engineering Research, 6(4), 2015, 425-433.
- [8] A. C. Reddy, "Parametric Optimization of Warm Deep Drawing Process of 2014T6 Aluminum Alloy Using FEA," International Journal of Scientific & Engineering Research, 6(5), 2015, 1016-1024.
- [9] A. C. Reddy, "Finite Element Analysis of Warm Deep Drawing Process for 2017T4 Aluminum Alloy: Parametric Significance Using Taguchi Technique," International Journal of Advanced Research, 3(5), 2015, 1247-1255.
- [10] A. C. Reddy, "Parametric Significance of Warm Drawing Process for 2024T4 Aluminum Alloy through FEA," International Journal of Science and Research, 4(5), 2015, 2345-2351.
- [11] A. C. Reddy, "Formability of High Temperature and High Strain Rate Superplastic Deep Drawing Process for AA2219 Cylindrical Cups," International Journal of Advanced Research, 3(10), 2015, 1016-1024.
- [12] A. C. Reddy, T. T. K. Reddy, M. Vidya Sagar, "Experimental characterization of warm deep drawing process for EDD steel," International Journal of Multidisciplinary Research & Advances in Engineering, 4(3), 2012, 53-62.
- [13] C.R. Alavala, "Finite Element Methods: Basic Concepts and Applications," PHI Learning Pvt. Ltd., New Delhi, 2008.
- [14] A. C. Reddy, "Evaluation of local thinning during cup drawing of gas cylinder steel using isotropic criteria," International Journal of Engineering and Materials Sciences, 5(2), 2012, 71-76.

Chennakesava R Alavala, Professor, Department of Mechanical Engineering, JNT University, Hyderabad, Telangana State, India.